EPR and NMR spectroscopy of spin-labeled proteins

Finiguerra, M.G.

Citation

Finiguerra, M. G. (2011, September 28). *EPR and NMR spectroscopy of spin-labeled proteins*. Retrieved from https://hdl.handle.net/1887/17881

Chapter IV

Paramagnetic NMR using spin-labeled proteins to study the structure of the complex between cytochrome f and plastocyanin

Abstract

Using site-specific spin-labeling in combination with paramagnetic relaxation enhancement (PRE) NMR spectroscopy, the physiological transient complex between cytochrome f (Cyt f) and plastocyanin (Pc) from cyanobacterium *Nostoc* sp. has been investigated and the interaction of Pc with five Cyt f cysteine mutants has been analyzed. In this work, the large magnetic dipolar interaction existing between unpaired electrons and nearby nuclear spins has been employed. The structure obtained has been compared to the results of a previous study performed using other NMR techniques, specifically pseudocontact shifts (PCSs) and chemical shift perturbations (CSPs). The conclusion of the present work is that a single structure does not satisfactorily represent the complex as previously proposed.

Introduction

In biomolecular research the understanding of the mechanism of biological processes at the molecular level is one of the main goals. Many biological processes involve protein-protein complexes. To understand how proteins interact to form a complex, and therefore how they react to undertake their functions, knowledge of the static complex structure alone, even at the atomic level, is not enough. A complete description of the protein-protein complex formation requires thinking of interacting proteins as 'objects in action'; thus, the study of protein dynamics becomes fundamental. The extension of the structure-function paradigm to include time as a fourth dimension, in addition to the three spatial dimensions, is required for the description of a complete protein-protein reaction mechanism.

In general, when two proteins meet each other to form a complex, they form a static complex if the affinity between the proteins is high. Conversely, if it is low they form a transient complex. The model of the process of protein-protein association, proved by kinetic and NMR studies recently reviewed[1], assumes that the complex formation begins with the proteins approaching by diffusion; they then start random collisions, which may develop into an initial association, the so-called *encounter complex*, which is in equilibrium with the final specific complex, - see Ubbink[1] and references therein (Fig. 4.1). In a transient complex the relative orientation of the proteins may vary from a single well-defined state to a highly dynamic cluster of orientations[2-10] which constitute the encounter complex[1]. Many studies[11-23] have provided evidence for the existence of encounter complexes both in transient protein-protein interactions and in protein-DNA interactions.
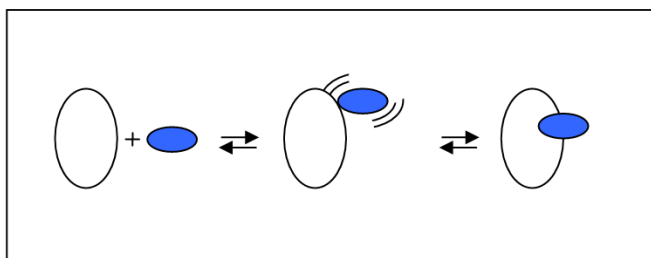
Figure 4.1 Protein complex formation model: the final single-oriented complex (right shape) is preceded by the ensemble of protein orientation middle, the so-called encounter complex[2].

To clarify the term "encounter complex", it is interesting to describe the evolution of its meaning over time, as reviewed by Volkov[11]. In 1968, Adam and Delbrück defined an *encounter complex* as two proteins occupying the same solvation shell as a result of a diffusion-driven collision process[24,25]. A later definition distinguished between a simple collision, happening when the distance of two proteins is small, and precisely equal to one hydration radius (*ca*. 2 Å), and an

actual encounter, *i.e.* the entire set of interactions from the initial collision to the final separation of the two proteins[26]. A refined version of the second definition further specifies an encounter complex as the state in which the protein touches the surface of the partner, via multiple microcollisions, and a specific active, *single-orientation complex* formed as a result of some of these collisions[25]. The character of transient protein complexes can vary from highly-dynamic to well-defined depending on the equilibrium between the encounter and the specific state. The transientness of protein complexes is related to their function. Some biological processes, such as electron transfer processes or processes related to signal transduction require the existence of transient protein complexes. In redox processes, usually one of the partners is a small carrier protein that shuttles electrons between its partners in the reaction chain.

The lifetime of complexes, in weakly bound electron transfer processes, can be very short (of the order of milliseconds), since it is essential that the complex rapidly dissociates. A balance between protein specificity and affinity is reached, and a high turnover can be achieved if both the association and dissociation rate constants of the complex (k_{on} and k_{off}, respectively) are high. If the lifetime of the complex is in the millisecond range, then the dissociation rate constant (k_{off}) is $\geq 10^3 s^{-1}$. The maximal association rate constant is the diffusion limit (10^7-10^9 M^{-1} s^{-1})[27-29]. These values for k_{on} and k_{off} imply a dissociation constant ($K_d = k_{off}/k_{on}$) in the μM–mM range. Conversely, the main characteristic of proteins performing their diverse set of functions through stable complexes is their ability to bind to other molecules specifically and tightly. For these protein complexes the specificity of the binding is determined by the complementary geometry of the protein surface (lock and key model); they are characterized by much lower dissociation rate constants (k_{off}) and, as a result, by long lifetimes.

In which way specificity is achieved has been a central question of studies for many years. Its answer is not completely known yet.[1-3,7-12,14,15,21,22,30,31,31]

Computational analysis of the crystal structures of redox protein complexes available revealed that fast dissociation is characterized by low geometric complementarity of the protein partners in the complex, which allows only a poor packing[32]. Protein-protein complexes are stabilized by a variety of non-covalent interactions, including van der Waals, electrostatic, hydrophobic interactions, net dipoles, intermolecular hydrogen bonds and salt bridges. Long-range electrostatic interactions are generally implicated in the early step of transient protein-protein association, while short-range hydrophobic interactions play a main role in the second step, allowing the protein to recognize its partners, to achieve specificity for carrying out a particular function, and to achieve stability. In electron transfer protein complexes, whose biological function requires them to be highly transient, a patch of hydrophobic residues is often found on the surface close to the active site, allowing for

protein-protein contact and, thus rapid electron transfer. Complete desolvation is not productive to carry out their function; therefore the hydrophobic patch usually represents a small fraction of the total surface of the protein and is surrounded by a ring of polar residues that promotes the dissociation of the complex[16,31]. Electron transfer partners react quickly and do not achieve high specificity, leading to low affinity and high k_{off}. In many cases electron transfer proteins have multiple partners reacting at the same binding site and, in those cases, a compromise in binding specificity is required. In other cases proteins form much more stable complexes, which require high specificity. The encounter complex is an integral part of the protein complex and plays different roles in the two complex formation types. A recent review[1] containing a summary of the relevant theoretical considerations and the discussion of the experimental results on the encounter state of protein complexes came to the conclusion that a complete description of protein complexes requires the study of both the well-defined, productive complex and of the dynamic encounter complex. To understand how specificity is achieved in weak and transient complexes requires therefore the ability to get insights into the interplay of the non-covalent interactions in the protein complexes, and the simultaneous knowledge of the productive complex and the dynamic encounter complex.

The complex between plastocyanin (Pc) and cytochrome f (Cyt f), studied in this thesis, is a transient complex involved in the electron transfer processes of the oxygenic photosynthesis[34-37]. The Cyt f is a transmembrane protein with a large soluble domain that is part of the cytochrome b_6f complex, which is embedded in the thylakoid membrane. In the photosynthesis of the oxygen-evolving photosynthetic organisms (plants, cyanobacteria and green algae), from the energetic point of view, the b_6f complex is situated
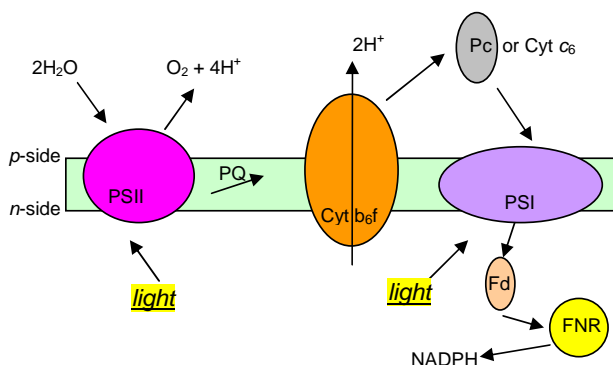
Figure 4.2 Schematic representation of the electron pathway in the oxygenic photosynthesis. The integral membrane protein complexes responsible for electron transport and proton translocation in oxygenic photosynthesis. The reaction centers of PSI (purple) and PSII (magenta), and the cytochrome b_6f complex (orange) are shown. Luminal (p) and stromal (n) -side soluble electron transfer proteins are plastocyanin (green) or cytochrome c_6, ferredoxin (pink), and ferredoxin-NADP reductase (yellow)[33].The idea and the layout of the figure was taken from ref. 33 in modified form.

between the two photosystems and transfers electrons from photosystem II-plastoquinone to plastocyanin-photosystem I (Fig. 4.2). Looking in more detail, Pc accepts an electron from the Cyt f of the cytochrome b_6f complex and transfers it to the pigment P700$^+$ from photosystem I[38]. Thus, Cyt f acts as an electron donor while P700$^+$ accepts electrons from reduced Pc. The cytochrome b_6f

complex and P700$^+$ are both membrane-bound proteins with exposed domains positioned on the lumen-side of the thylakoid membrane of cyanobacteria or chloroplasts (for plants and eukaryotic algae) in which the Pc is located. In the same cellular space another soluble protein, the cytochrome c_6, is also located, serving, in certain conditions, as an alternative electron carrier.

While Pc is the only electron carrier in higher plants and the cytochrome c_6 is the only one in some cyanobacteria[39], certain eukaryotic algae and cyanobacteria are capable of synthesizing either Pc or cytochrome c_6, depending on the availability of copper in the culture medium[40-43]. The two proteins, Pc and Cyt c_6, have different structures but carry out the same physiological function, the transfer of electrons from the cytochrome b_6f complex to PSI.

Besides being interesting for its physiological function, the Cyt f-Pc complex, due to the large amount of data available, represents an excellent model system for the understanding of transient interactions between proteins[44,45]. The lifetime of this type of complex is about 1 ms. Previous studies suggested that, depending on the organism from which it is derived (i.e. plants, algae or cyanobacteria), the kinetics of the Cyt f - Pc complex may vary greatly, highlighting in some cases differences in the reaction mechanism between *in vivo* and *in vitro* experiments[31,46-54] Extensive structural investigation of the transient Cyt f-Pc complex showed also differences in the orientations of the two proteins from different organisms in the complex[2,4,31,44,46,49,55-59]. This complex being transient, it requires the analysis of the time-dependent dynamics of the protein complex formation and the experimental characterization of the encounter complex. Recent studies on different protein complexes showed that a computational approach associated with restraints derived from experimental data, is a very promising way for the study of the elusive encounter complex[1,14,23]. Several spectroscopic techniques can be used for experimental investigations, including paramagnetic relaxation enhancement (PRE), pseudocontact shift and residual dipolar coupling NMR.

The PRE technique provides long-range distance information (up to 25-35 Å)[61]. Distances between a paramagnetic centre containing unpaired electrons, like a spin label or a metal ion, and a nucleus can be determined from the increased nuclear T_2 relaxation rate. The effect of the unpaired electron of a spin label on the relaxation rates is very strong at short distances between the nucleus and the paramagnetic centre, and it falls off with the sixth power of the distance. The PRE technique can detect conformations that represent only a small percentage of the complex. In this way, information on the surface area sampled by the protein partner can be obtained. The PRE is an average over all conformations, so it may represent either a heavily populated state far from the paramagnetic centre or a lowly populated state at short distance. Distinguishing between these two situations is impossible[1].
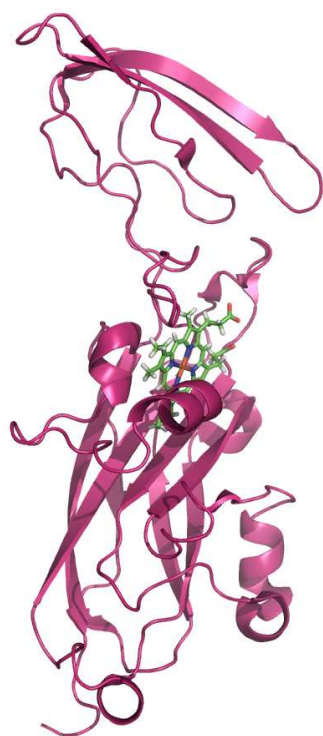
Figure 4.3 Three-dimensional structure of Cyt *f*. The protein is shown in pink and the haem, with the Fe in the center (red), is shown as sticks. The figure has been generated from the NMR structure of the complex between Pc and Cyt *f* from the cyanobacterium *Nostoc* sp. PCC 7119 (PDB entry 1tu2)[56]. The figure has been made with PyMOL v 0.98[60].

The larger protein used in this investigation is the truncated Cyt *f* subunit (Fig. 4.3), consisting of a ca. 28 kDa N-terminal soluble domain that in the cyanobacterium *Nostoc* sp. PC 7119 is anchored to the membrane by a C-terminal helix[62]. It is an atypical *c*-type cytochrome, having an unusual haem axial coordination (the N-terminus being one of the haem ligands). The secondary structure is mainly β-sheet.
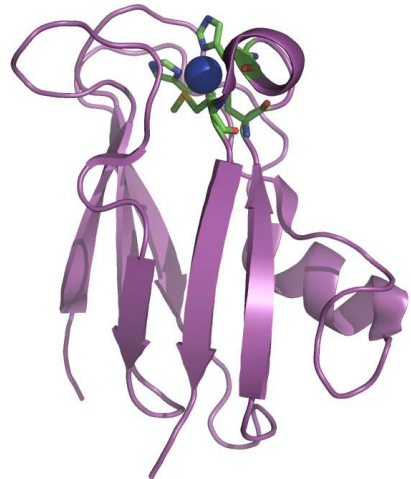
The partner protein, Pc, is a small (11 kDa) type I copper protein with the metal ion coordinated by two histidines, one cysteine and one methionine[48] (Fig. 4.4). Two functional regions, the hydrophobic and the electrostatic patch, have been identified on Pc. The first one, site 1, is positioned at the so-called north end surface of the molecule surrounding a copper-ligand histidine and is involved in the electron transfer[2]. The second one, site 2, is situated at the 'east side' of the molecule, playing in some cases, like in plants, a key role in electrostatic interactions with the redox partners[62]. Generally, the structures of Cyt *f* and Pc are well conserved among plants, algae and cyanobacteria, although differences are observed in the distribution of charges on both proteins, permitting in all cases electrostatic attractions with the partner protein in the complex.[33,48,63,64] In plants and *P. laminosum* the Pc is an acidic protein (pI = 5.5 and pI = 5.0, respectively), while in Pc from the cyanobacterium *Nostoc*, it is basic (pI = 8.8). A comparison between the amino acid sequences of the Pc partner, Cyt *f* from *P.*

laminosum and Cyt *f* from *Nostoc*, reveals a high similarity, with the exception of a range of about sixty residues, found between position 170 and 230, which correspond to the small domain of the soluble part of the protein. The surface charge of *Nostoc* Cyt *f* is different from that of *Phormidium* Cyt *f*, and is involved in the interactions within the complex, even though this effect is much more evident *in vitro* then *in vivo*[65]. Differences in surface charge distributions are reflected in the modality of

approach between the two proteins and in their mutual orientation in the complex.[4,55,56,65]

In the Cyt *f*-Pc complex from cyanobacterium *Nostoc sp.*, significant structural differences have been found with respect to equivalent complexes from other sources[2,56]. The three-dimensional structure of the *Nostoc* Pc-Cyt *f* complex has been characterized by NMR spectroscopy[56] using intermolecular pseudo-contact shifts caused by the heme iron and chemical shift perturbation data, thus revealing that this complex adopts a conformation similar to the one found in plants, which is in the side-on binding mode, but with opposite charge[2]. The interface of the *Nostoc* Pc-Cyt *f* complex is similar to that of the cyanobacterium *Phormidium laminosum* complex. The latter, though, shows an atypical head-on orientation[4,65]. At the interface region of the complex, the

Figure 4.4 Three-dimensional structure of Cu-Pc. The copper atom is shown as blue sphere and the four ligands, a cysteine, methionine and two histidines, are shown as sticks. The figure has been generated from the crystal structure of plastocyanin from the cyanobacterium *Anabaena variabilis* (PDB entry 2gim)[66].

binding site involves the hydrophobic areas close to the metal sites in both proteins[56]. But whereas in *Phormidium* the interaction in the complex is weakly salt dependent, in *Nostoc* it varies greatly with the ionic strength; in fact, the binding constant for the complex of *Nostoc* at low ionic strength becomes an order of magnitude larger compared to the one at physiological ionic strength[65]. A mutagenesis study of the complex demonstrated that Pc protein dictates the specificity of the electrostatic interaction. Specific short-range electrostatic interactions are present as well and, as already mentioned above, these are due essentially to the Cyt *f* [67].
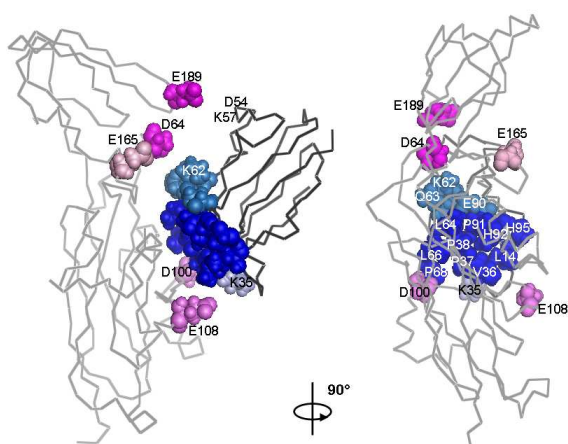
In Cyt *f* five acidic residues (pink residues in figure 4.5) play a relevant role in the electrostatic interactions with the positive groups of Pc. These residues are: Asp-64 and Glu-189, located on the small domain region of Cyt *f*, containing an acidic patch; Asp-100 and Glu-108, which are on the large domain; and Glu-165, located near the hydrophobic patch[56]. The charged residues are located at the border of a group of 20 residues (some of them being at least partially

buried) involved in the recognition site, most of which are hydrophobic or uncharged polar. Five aromatic residues are present on this patch and three of them, specifically Tyr 1, Phe 3, and Tyr 102, constitute about 31% of the recognition surface of Cyt *f*. Six proline residues (which are amino acids with very low propensity in protein-protein interfaces)[68-70] are located in the interface. The inability of Pro to form hydrogen bonds may be employed to limit the affinity in such complex[56]. Furthermore, 4.3% of the recognition sites of the complex are derived from the polar, uncharged amino acid glutamine, which, surrounding the hydrophobic patch, may improve dissociation by facilitating resolution of the interface, as suggested by Crowley and Ubbink[31].

In Pc, the interface region comprises 14 residues (Fig. 4.5). Ten from the hydrophobic patch (Leu-14, Val-36, Pro-37, Pro-38, Leu-64, Met-66, Pro-68, Pro-91, His-92, and Ala-95, indicated in blue in Fig. 4.5), three from the nearby region of site 2 (Lys-62, Gln-63, and Glu-90), and the Lys-35 which is adjacent to the hydrophobic patch[56]. A second, minor recognition site on Pc corresponds to residues Asp-54 and Lys-57, interacting with the acidic patch of the above mentioned small domain of the Cyt *f* [56].

Kinetic studies of the *Nostoc* Cyt *f*-Pc complex to investigate the contribution of the charged residues to the interaction energy and to identify specific short-range electrostatic interactions between charged residues have been carried out[67]. To this purpose a series of site-directed mutants of Cyt *f*, neutralizing the charge of negative residues with alanine or reverting it upon substitution by lysine, were

Figure 4.5 Nostoc Cyt *f* – Pc interface. In pink, the five Cyt *f* residues playing a relevant role in the electrostatic interactions with the positive group of Pc (dark pink: residues located on the small domain of Cyt *f*; light pink: residue close to the hydrophobic patch; medium pink: residues located on the large domain). In blue, the 14 Pc residues on the interface region (dark blue: the 10 hydrophobic residues from the hydrophobic patch; medium blue: residues located in site 2; light blue: basic residue 35 close to the hydrophobic patch). On the left figure, adjacent to E189 of Cyt *f*, the positions of the two Pc residues of the second recognition site are also shown[56].

constructed. The effects of mutations on the kinetics of electron transfer to wild-type and mutant forms of Pc were measured by laser flash absorption spectroscopy. The results showed that in the *Nostoc* complex the main contribution to the electrostatic interaction with Pc in the complex is provided by the small domain of Cyt *f*. The Cyt *f* mutants, with some negative charges replaced with neutral residues, revealed an apparent electron transfer rate constant with wild-type Pc similar to (or

slightly higher than) that of the wild-type species. Mutants, in which negative charges were replaced by positive residues exhibited instead a significantly lower reactivity. Furthermore, in contrast with the more defined surface found in Pc[71], a wide electrostatic area was involved, as the result of an additive effect of multiple specific interactions. As a consequence the substitution of a single charged residue in the Cyt *f* does not promote drastic changes in the interaction with the Pc. A similar outcome was obtained by mutating specific residues in *Phormidium* Cyt *f* [55]. Different results were obtained from the analysis of the interaction of Cyt *f* (wt) with site-directed mutants of charged residues in the positive patch of *Nostoc* Pc[71]. In that case, the neutralization or the charge inversion of the key residues promoted significant changes in complex formation and electron transfer, suggesting that the specificity of the Cyt *f*-Pc interaction is mainly determined by the electrostatic features of Pc. These results are in agreement with the particular orientation of the two partners described in NMR studies[56]. The parallel kinetic behaviour showed that Pc uses the same surface area to interact with both its redox partners, Cyt *f* and Photosystem I (PSI)[67,71,72]. The electrostatic patch enhances the association rate, and the hydrophobic area is used for electron transfer.

Several structural studies on electron transfer (ET) complexes like that between Pc and Cyt *f* have been performed, as recently reviewed[1]. Some ET complexes appear to be mostly specific[2,11,73], while others are completely or mainly non-specific[3,6,9,10,15,74], and the encounter state is the most populated form. The structure of the ET *Nostoc* Pc-Cyt *f* complex was found to be well-defined, as it is in the case of plants[2,56], in contrast with the highly dynamic structures found in the case of *P. laminosum*[4] and of *Prochlorothrix Hollandica*[58]. All these complexes, which are transient, were studied using paramagnetic NMR spectroscopy, which is a powerful technique for *in vitro* studies of structure and dynamics of soluble biological macromolecules. If a nucleus approaches a paramagnetic tag like a stable free radical or a paramagnetic metal ion, a shift of the nuclear resonance or a change in its relaxation time results. Different paramagnetic NMR techniques can be used for experimental investigations, including paramagnetic relaxation enhancement (PRE), pseudocontact shift (PCS) and residual dipolar couplings (RDCs). In the work of Diaz-Moreno and collaborators, the *Nostoc* Pc-Cyt *f* complex was studied using PCSs and chemical shift perturbation (CSP)[56]. In the present work, we use PRE NMR with the purpose of complementing this study, acquiring independent constraints for complex structure determination, and getting information concerning the encounter complex. Paramagnetic Relaxation Enhancement is isotropic and inversely dependent on the sixth power of the distance between nucleus and paramagnetic centre, while the PCS depends on the orientation of nucleus within the frame set by the magnetic susceptibility tensor, and is inversely dependent on the third power of distance between nucleus and

paramagnetic centre. The observable RDC, on the other hand, does not depend on the nucleus-tag distance. All these techniques, therefore, provide different views of the complex dynamics[14,75].

The PRE technique provides long-range distance information (15-24 Å). Distances between a paramagnetic centre containing unpaired electrons, like a spin label, can be determined from the increased T_2 relaxation rates. The effect of an unpaired electron on the relaxation rate is very strong at short distances. Consequently, the PRE technique is able to detect also conformations representing only a small percentage of the complex in which the paramagnetic centre is close to the active nuclei.

When spin labels are attached to different positions on the protein surface, it is possible to acquire information about the surface sampled by the partner protein in the encounter complex[11,23]. Such effects are, however, an average over time and space. Hence, the information obtainable from this technique could be caused by either a heavily populated state characterized by long-distance interactions, or by a lowly populated state with short distance interactions; it is not possible to distinguish between these two situations[1]. Still, it must be taken into account that an important advantage of this technique is that it also allows to study sparsely populated conformational ensembles in solution[75], as it happens in some cases for the encounter complex. This method has been extensively used to demonstrate the existence of the encounter complex by Clore and coworkers[13,76] and Ubbink and coworkers[11,23].

In the present work, therefore, we aim to investigate the structural aspects of the transient complex between Pc and Cyt *f* from the cyanobacterium *Nostoc* sp. PC 7119 (formerly *Anabaena variabilis*) using the PRE technique, in combination with site-directed spin labelling (SDSL). The Pc has been uniformly ^{15}N labeled and was used to form a complex with its physiological partner, the Cyt *f*. The results of this study indicate that the Cyt *f* – Pc complex cannot be described only as a single structure, but must be depicted as the equilibrium between a specific and an encounter complex, a view that was recently suggested also for the Pc-Cyt *f* complex from other species[58], as well as for a complex between Cyt *f* and cytochrome c_6[77].

Materials and Methods

Site Directed Spin Labeling of Cyt *f*

- *Mutagenesis*

The pEAF-wt[71] expression plasmid encoding the soluble domain of Cyt *f* from *Nostoc* sp. PCC7119 was kindly provided by Prof. Miguel De la Rosa, Instituto de Bioquímica Vegetal y Fotosíntesis, Universidad de Sevilla, Spain. To avoid changes in the p*I*, which could affect the

protein-protein interactions, only neutral amino acid residues (N, Q, S, A) were replaced by cysteine. In order to prepare the single-cysteine Cyt f variants Q7C, A63C, N71C, Q104C and S192C, mutations were introduced in the Cyt f gene using the Quik Change[TM] polymerase chain reaction protocol (Stragene, La Jolla, CA) with the plasmid pEAF-wt as a template and the primers indicated in Table 4.1. All constructs were verified by DNA sequencing.

Table 4.1. **Primers used in site–directed mutagenesis of Cyt *f*. Codon-changing (bold italic underlined) and silent (highlighted) mutations are indicated.**

Q7C (34 bp; restriction enzyme: ApaL I)

forward   5'– GCATATCCTTTCTGGGCGCAG***TGC***ACTTACCCAG – 3'

reverse   3'– GACCCATTCA***CGT***GACGCGGGTCTTTCCTATACG – 5'

A63C (36 bp; restriction enzyme BstX I)

forward   5'– CCAGCGTCCAACAAGTTGGT***TGC***GATGGCTCTAAGG – 3'

reverse   3'– GGAATCTCGGTAG***CGT***TGGTTGAACAACCTGCGACC – 5'

N71C (31 bp; restriction enzyme: Sty I)

forward   5' – GGCTCCAAGGTCGGCTTA***TGC***GTCGGTGCTG – 3'

reverse   3'– GTCGTGGCTG***CGT***ATTCGGCTGGAACCTCGG – 5'

Q104C (32 bp; restriction enzyme: Bgl I)

Forward   5' – CGGCGATGTTTACTTC***TGC***CCCTACGGCGAAG – 3'

Reverse   3' – GAAGCGGCATCCC***CGT***CTTCATTTGTAGCGGC – 5'

S192C (36 bp; restriction enzyme: Sal I)

Forward 5'– GGCGAAGATGGT***TGC***GTTAAATATTTAGTCGACATC – 3'

Reverse 3' – CTACAGCTGATTTATAAATTG***CGT***TGGTAGAAGCGG – 5'

For A63C and N71C a silent mutation was designed to introduce an extra BstX I and Sty I restriction site respectively, located close to the *5'* end of the primer (Table 4.1). In the case of the S192C mutant a Sal I restriction site was introduced at the *3'* end of the primer (Table 4.1). The mutagenesis for preparing Q7C and Q104C mutant has been described previously[78]: to introduce a cysteine instead of the asparagines at the position 71 the direct primer (see table 4.1) was designed inserting at the same time the Sty I restriction site next to the *5'* end of the primer. Analogously, to introduce a cysteine instead of the glutamine at the position 104 the direct primer was designed, inserting an extra Bgl I restriction site respect to the wild type.

Protein production and purification

- *Cytochrome f variants*

To improve the yield of holocytochrome *f* and promote the correct insertion of the haem group, *E. coli* strain MV1190 (Bio-Rad) was co-transformed with plasmids pEC86[79] and (mutated) pEAF plasmid. The cells were plated on Luria-Bertani (LB) medium plates and incubated at 37° C for 24 hours. This medium and those mentioned below were supplemented with 20 mg/L ampicillin (amp) and chloamphenicol (cam). Several pre-cultures were prepared in 100 mL flasks with 20 mL of LB medium and incubated at 37 °C and 250 rpm for 5-6 hours. The pre-cultures with the highest OD_{600} were used to inoculate 1.7 L (in 2 L Erlenmeyer flasks) of LB, ratio 1:100. The cultures were incubated at 25 °C and 150 rpm for more a 72 h under semi-anaerobic conditions and high antibiotics pressure by adding further amp and cam after 20 h and 40 h. Expression was induced 20h after the inoculation of the large culture using 1 mM IPTG (isopropyl-β-thiogalactopyranoside). More than 80 h after the induction the cultures appeared brown for the presence of the Cyt *f*. The cells were harvested by centrifugation and the periplasmic fraction was extracted by osmotic shock[80]. The pink water fraction (about 200 mL *per* 1.7 L of culture), tested for the presence of Cyt *f* by UV/vis analysis, was dialyzed against 2 L of 5 mM Tris-HCl buffer, pH 8 and 3 mM dithiothreitol (DDT). The resulting dialysate was cleared by centrifugation and loaded on a DEAE column equilibrated in the same buffer. Elution was performed with a gradient of 20–500 mM NaCl and 3 mM DTT. The fraction containing the Cyt *f* was concentrated and loaded on a gel-filtration (G75 Superdex) column and eluted in the same buffer containing 150 mM NaCl. The protein fractions were pooled, concentrated, dialysed against 5 mM Mes, pH 6 and 3 mM DTT and loaded on a DEAE column equilibrated in the same buffer. The Cyt *f* was eluted with a gradient 0-500 mM NaCl. Pure fractions showed a A_{280}/A_{556} of 1.3 under reducing conditions. The protein concentration was determined using $\varepsilon_{556} = 31.5$ mM^{-1}cm^{-1}. The yield of the pure proteins was 36 mg/L for Q7C, 16 mg/L for Q104C, 14 mg/L for N71C, 18 mg/L for S192C and 2.4 mg/L for A63C, referred to the volume of the culture.

- *Plastocyanin*

Uniformly ^{15}N-labeled Pc (^{15}N-Pc) was produced in *E. coli* JM109 transformed with pEAP-wt[81]. A 10 mL LB/amp (100 μg/mL) pre-culture was incubated at 37°C for 8 h. Then 1 mL was used to inoculate 500 mL of room temperature ^{15}N-labeled OD2 Silantes media purchased from *Buchem* B.V. (formerly ARC Laboratories B.V. – The Netherlands) containing 100 μg/mL AMP and 1 mM copper citrate at pH 6. The culture was incubated at 37 °C/225 rpm overnight to $OD_{600} = 2.5$. Isolation and purification of the protein was performed as described previously[81]. For *Nostoc*

Pc, a ratio A_{278}/A_{598} of 1.0 of the oxidized protein indicated sufficient purity for characterization by NMR and further applications[65]. The solution containing the ^{15}N-labeled Pc protein was concentrated to the required volume by ultrafiltration (Amicon, YM3 membrane). The protein concentration was determined by absorption spectroscopy using an ε_{598} of 4.5 mM^{-1} cm^{-1} for the oxidized forms of ^{15}N-Pc[65]. The yield of the pure proteins was 7 mg *per* litre of culture.

Zn-substitution of Pc

For the study of the interaction of Pc with Cyt *f* without interference from possible electron transfer reactions and to avoid the paramagnetism of the Cu(II), the Cu in Pc was replaced by the redox inactive substitute Zn(II). The Zn substitution was performed in a way similar to the one previously described for the incorporation of Cd into Pc[82], with the following modifications. To produce Pc(Zn), 6 mg of oxidised Pc(Cu) were concentrated to a volume of 0.5 mL. The solution containing the concentrated protein was kept on ice. A solution of 200 mM KCN in 500 mM Tris-HCl pH 7 (200 μL) was slowly added to the protein solution. The blue colour gradually disappeared. The solution was left on ice for 10 min. Then, 1 mM $ZnCl_2$ in 50 mM MES pH 7 (buffer A) was added to the sample to get a total volume of 1-1.5 mL. The solution was loaded on a PD10 column, equilibrated with buffer A, and eluted with up to 3.5 mL of buffer A. Fractions of 0.5 ml with the Zn protein were collected and the absorption at 280 nm was measured. To avoid Zn precipitation, the solution of the fractions containing the protein was first exchanged against water, then against 10 mM sodium phosphate buffer, at pH 6.0. The protein was concentrated to 1 mM. The concentration was checked at 280 nm using an extinction coefficient ε_{280} of 5.1 mM^{-1} cm^{-1}.

Spin-labelling of Cyt f mutants

Before adding the spin labels the excess DTT, used to avoid disulfide bridge formation, was removed from the Cyt *f* cysteine mutant solution, by several concentration/redilution cycles with degassed 10 mM sodium phoshate buffer pH 6. To avoid reduction of the disulfide group by the Fe(II) haem resulting in loss of the spin label, the protein was oxidized by adding a 100-fold excess of $K_3[Fe(CN)_6]$ to the solution before adding a 10 fold excess of MTSL [(1-Oxyl-2,2,5,5,-tetramethyl-3-pyrroline-3-methyl)-methanethiosulfonate] or MTS [(1-Acetyl-2,2,5,5,-tetramethyl-3-pyrroline-3-methyl)-methanethiosulfonate], both purchased from Toronto Research Chemicals, Ontario, Canada (Figure 1, Chapter I). Stock solutions of 0.1 M MTSL or MTS in DMSO were used. The solution containing the protein and the spin label was left for 2 h at room temperature and then overnight at 4° C. The excess $K_3[Fe(CN)_6]$ and MTSL were removed by several concentration/redilution cycles with degassed 10 mM sodium phosphate buffer pH 6. The degree of

labeling of the protein was estimated by EPR experiments[11]. The percentage of bound Pc was calculated to be 27% using $K_a = 16 \times 10^3$ M^{-1} [56]. This fraction was estimated on the basis chemical CSP and PCS values, by comparison with the *w.t.* values, for which the binding curves in known[56].

NMR spectroscopy

The NMR samples contained 1 mM of 1:1 complex of ^{15}N Pc and Cyt f – MTSL or Cyt f – MTS in 20 mM sodium phosphate pH 6.0, 6% of D$_2$O for lock, and 0.1 mM CH$_3$CO^{15}NH$_2$ as internal reference. The pH of the sample was adjusted to the pH 6.00 using small aliquots of 0.1 M HCl or 0.1 M NaOH, as required. All measurements were performed at 301 K on a Bruker DMX600 spectrometer equipped with a triple-resonance TXI-Z-GRAD probe (Bruker, Karlsruhe, Germany). Performing 2D [^{15}N, ^{1}H] HSQC experiments, spectra were obtained with 1024 and 256 complex points in the direct and indirect dimensions, respectively, and spectral widths of 32 ppm (^{15}N) and 16 ppm (^{1}H). All data were processed with AZARA 2.7 [83] and analysed in ANSIG for Windows[84,85]. Assignments of the ^{15}N and ^{1}H nuclei of Pc were based on 3D NOESY and TOCSY-HSQC spectra (not shown) and are listed in Appendix A. Several Pc amides were either not observed or not analysed due to spectral overlap.

Determination of distance restraints

The unpaired electron of the spin label enhances the relaxation rate of the nuclei in its proximity by the magnetic dipolar interactions. The magnitude of the effect, reflected in line broadening, depends on the distance, providing structural information[86]. In the present work, the PRE was calculated using equation 4.1[86]:

$$\frac{I_{para}}{I_{dia}} = \frac{R_{2,dia}\exp(-tR_{2,para})}{R_{2,dia}+R_{2,para}} \qquad \text{(Eq. 4.1)}$$

where I_{para} and I_{dia} are the resonance intensity of an amide group in [^{1}H, ^{15}N] HSQC spectra for Pc in the complex containing Cyt f – MTSL and Cyt f – MTS, respectively; $R_{2,dia}$ is the transverse relaxation rate of Pc amide protons in the complex with Cyt f – MTS; $R_{2,para}$ is the paramagnetic contribution to the relaxation rate (PRE) and t is the INEPT evolution time of the HSQC (9 ms). For residues whose resonances disappear in the paramagnetic spectrum, the maximal I_{para} value was set to the noise level of the spectrum. The I$_{para}$ / I$_{dia}$ ratios were normalized as previously described[11]. For all amide protons, the $R_{2,dia}$ was determined from the HSQC peaks of the Pc in the complex with Cyt f – MTS. The FIDs in the HSQC spectra were zero-filled up to 2048 and 512 complex points in

the direct and indirect dimensions, respectively, and processed with a 2 Hz line-broadening exponential multiplication window-function in the ^{1}H dimension. For each peak the width at half-height ($\Delta v_{1/2}$) in the proton dimension was extracted from a Lorentzian fit using MestRec-C 4.8.6.0 (Mestrelab Research S.L., Santiago de Compostela, Spain). After correction for the artificial line-broadening, the $\Delta v_{1/2}$ was used to calculate $R_{2,dia}$ ($R_{2,dia} = \pi \Delta v_{1/2}$). $R_{2,para}$ was then obtained by a fit of data to equation 4.1. The PREs values were converted into distances using equation 4.2:

$$r = \sqrt[6]{\frac{\gamma^2 g^2 \beta^2 f_b f_e}{20 R_{2,para}}(4\tau_c + \frac{3\tau_c}{1+\omega_h^2 \tau_c^2})} \qquad \text{(Eq. 4.2)}$$

where r is the distance between the unpaired electron of the MTSL bound to the Cyt f and a given amide proton of Pc; γ is the gyromagnetic ratio of ^{1}H; g is the electronic g-factor; β is the Bohr magneton; f_b and f_l are fraction Pc bound and fraction Cyt f spin labeled, respectively; τ_c the correlation time of the electron-nucleus vector and ω_h is the proton Larmor frequency. The τ_c values were determined from EPR spectra of each Cyt f mutant in the presence of Pc (see Results).

Docking

The intermolecular distance restraints obtained from the PREs were employed to guide the docking of Pc onto Cyt f. The distance restraints were categorized in three classes[86]. The spin label-amide distances for residues for which the resonances disappeared in the paramagnetic spectrum were restrained only with an upper limit. For those not affected by MTSL only a lower limit was set. Finally, for the residues affected by the spin-label and for which resonances were observed in the paramagnetic spectra the distances were restrained with both upper and lower limits. Restrained rigid-body docking of the protein molecules was carried out using Xplor-NIH 2.13[87] as described previously[2,4,11,49,56]. Dr. A. Volkov is kindly acknowledged for performing these computations. The coordinates of Cyt f and Pc were taken from the NMR structure of the complex (PDB entry 1tu2[56]) and from the crystal structure (PDB entry 2GIM[66]), respectively.
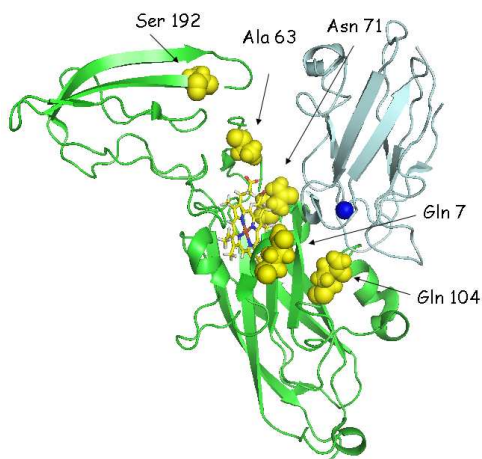
The spin label is very mobile because of the possible rotation around the five single bonds of the chain linking the protein to the pyrrolidinic ring which contains the paramagnetic nitroxide, (see Introduction, Fig. 2). This mobility was accounted for in the calculations by selecting four orientations from the sterically allowed conformers, and obtaining, for each mutant, the averaged position of the oxygen atom of MTSL. As reported in the literature, using a greater number of orientations did not modify the final result[11,88].

The coordinates of Cyt *f* were fixed, whereas Pc was placed at a random position and left to move under the action of two energy terms, the PRE restraints and van der Waals repel forces, which were defined for the protein atoms but set to zero for the spin labels. After that, the 30 – 40 best structures were further minimised in energy allowing only side-chain dynamics, with the repel function now also including the spin labels. Finally, the whole docking procedure was repeated till the lowest energy was obtained.

Results

The complex between Pc and Cyt *f* from cyanobacteria *Nostoc* sp. PC 7119 (formerly *A. variabilis*) has been investigated by NMR, using the PRE technique in combination with SDSL. The structure of the Pc-Cyt *f* complex was previously investigated by Diaz-Moreno *et al.*[56]. In that study pseudo-contact shifts of Pc amide resonances, caused by the haem iron, and the chemical-shift perturbation data were used to determine the structure of the complex (PDB entry 1tu2). The aim of the present work was to obtain independent structural restraints for validation and refinement of the structure as well as information about the encounter complex.

Five variants of Cyt *f* were created in which a single surface exposed residue was replaced by a cysteine for attachment of a thiol specific paramagnetic spin label (MTSL), or its diamagnetic homologue (MTS). The Cyt *f* does not contain other free thiol groups, making the engineered cysteine residue a unique position for spin label linkage. The positions 7, 63, 71 and 104 are in proximity of the haem. Residue 192 is more distant, positioned on the small domain of Cyt *f* (Fig. 4.6). Table 4.2 lists the distances between the mutated residues and the haem iron of the Cyt *f*, or the Cu of the Pc, using the published structure of the complex.


Figure 4.6 Ribbon model of the Cyt *f*-Pc complex from *Nostoc*. The residues represented in space filling have been replaced, one at time, by cysteine. Cyt *f* is shown in green, with the haem sticks. Pc is in light blue, with the copper shown as a blue sphere. Coordinates from PDBdata bank, accession codes 1tu2[56].

Table 4.2. Distances (Å) from the C_α atom of the mutated residue to the haem iron and copper in the Cyt *f* –Pc complex (ref 22)

Residue	Haem	Cu
N71C	10.0	18.0
Q104C	15.4	13.5
Q7C	12.0	14.1
A63C	12.7	19.0
S192C	24.7	30.7

All Cyt *f* variants could be produced in the same recombinant expression system as for w.t. Cyt *f*. To avoid interference from electron transfer reactions and paramagnetism of Cu(II) the Pc copper ion was substituted with Zn(II) (see material and methods).

PREs in the ^{15}N ZnPc - Cyt f-MTSL complexes

To produce an intermolecular paramagnetic relaxation enhancement on the amide protons of the ^{15}N-Pc, the spin labels were linked to the cysteine residues on Cyt *f*. Previous EPR[89] and NMR[86] spectroscopy studies have demonstrated that nitroxide spin labels typically perturb only negligibly the structures of soluble proteins. To measure the PRE accurately, parallel labeling with paramagnetic and diamagnetic compounds of very similar structures was performed[11,90]. Hence, the spin labels MTSL [(1-Oxyl-2,2,5,5,-tetramethyl-3-pyrroline-3-methyl)-methanethiosulfonate] (see Figure 1, Chapter I), and its diamagnetic homologue MTS [(1-Acetyl-2,2,5,5,-tetramethyl-3-pyrroline-3-methyl)-methanethiosulfonate], in which the oxygen on the nitroxide of MTSL is replaced with an acetyl group, were used.

For each Cyt *f* variant, ^{15}N-^{1}H HSQC spectra were acquired of ^{15}N-Pc in complex with Cyt *f* labeled with MTSL or MTS, under identical conditions. The resonance intensities (based on peak heights) were measured for all amides to obtain I_{para} and I_{dia}. From the ratio of these values, as well as the linewidth of the peaks in the Cyt *f* MTS spectra ($R_{2,dia}$), the PRE ($R_{2,para}$) was derived (eq. 4.1 in material and methods). The normalized I_{para} / I_{dia} ratios are shown in Fig. 4.7 and the data are summarized in Tables 1 in Appendix B.
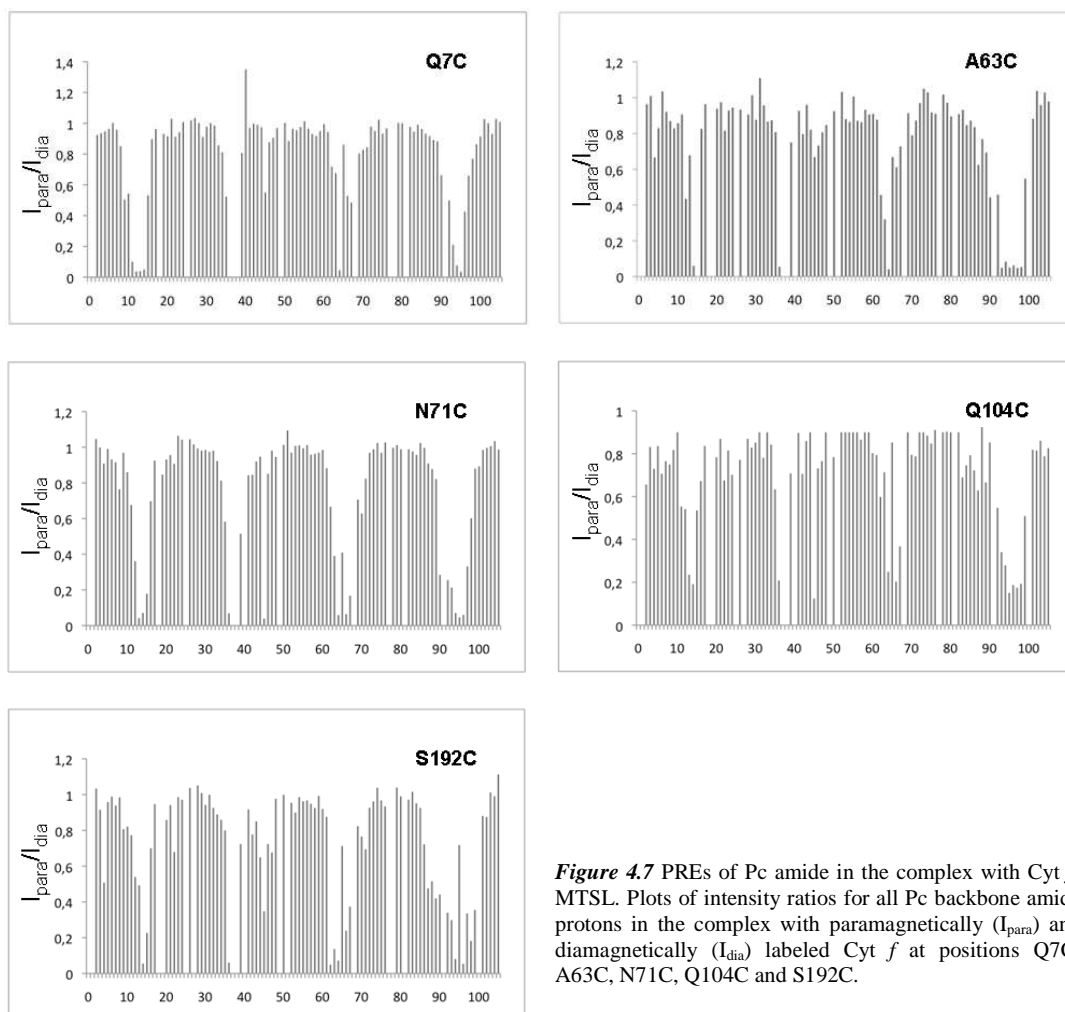
Figure 4.7 PREs of Pc amide in the complex with Cyt *f*-MTSL. Plots of intensity ratios for all Pc backbone amide protons in the complex with paramagnetically (I_{para}) and diamagnetically (I_{dia}) labeled Cyt *f* at positions Q7C, A63C, N71C, Q104C and S192C.

The relaxation effects have been visualized in Fig. 4.8. This figure shows the surface of Pc coloured according to the size of the observed PREs. Surprisingly all Cyt *f* variants affect the same region of the Pc surface. This is remarkable, because each spin label would be expected to enhance relaxation of nuclei in different regions and to different degrees if the complex were in a single conformation. Fig 4.6 shows that the spin label positions are spread around the interface of the Cyt *f* - Pc complex. The chemical shift perturbations observed for Pc bound to the Cyt *f*-MTS variants are quite comparable to that of w.t. Cyt *f* [56] (data not shown), indicating that affinity and interface were not affected by the introduction of the SL. Only for variants A63C some deviations were observed, suggesting small changes in binding in this complex. The general effects observed on the hydrophobic patch of Pc and surrounding region cannot be explained by a single orientation and strongly suggest the complex is dynamic to some extent. Furthermore, it must be underlined that on

the Pc always the same interface is affected, suggesting that Pc uses this area to interact with a large portion of the Cyt *f* surface.
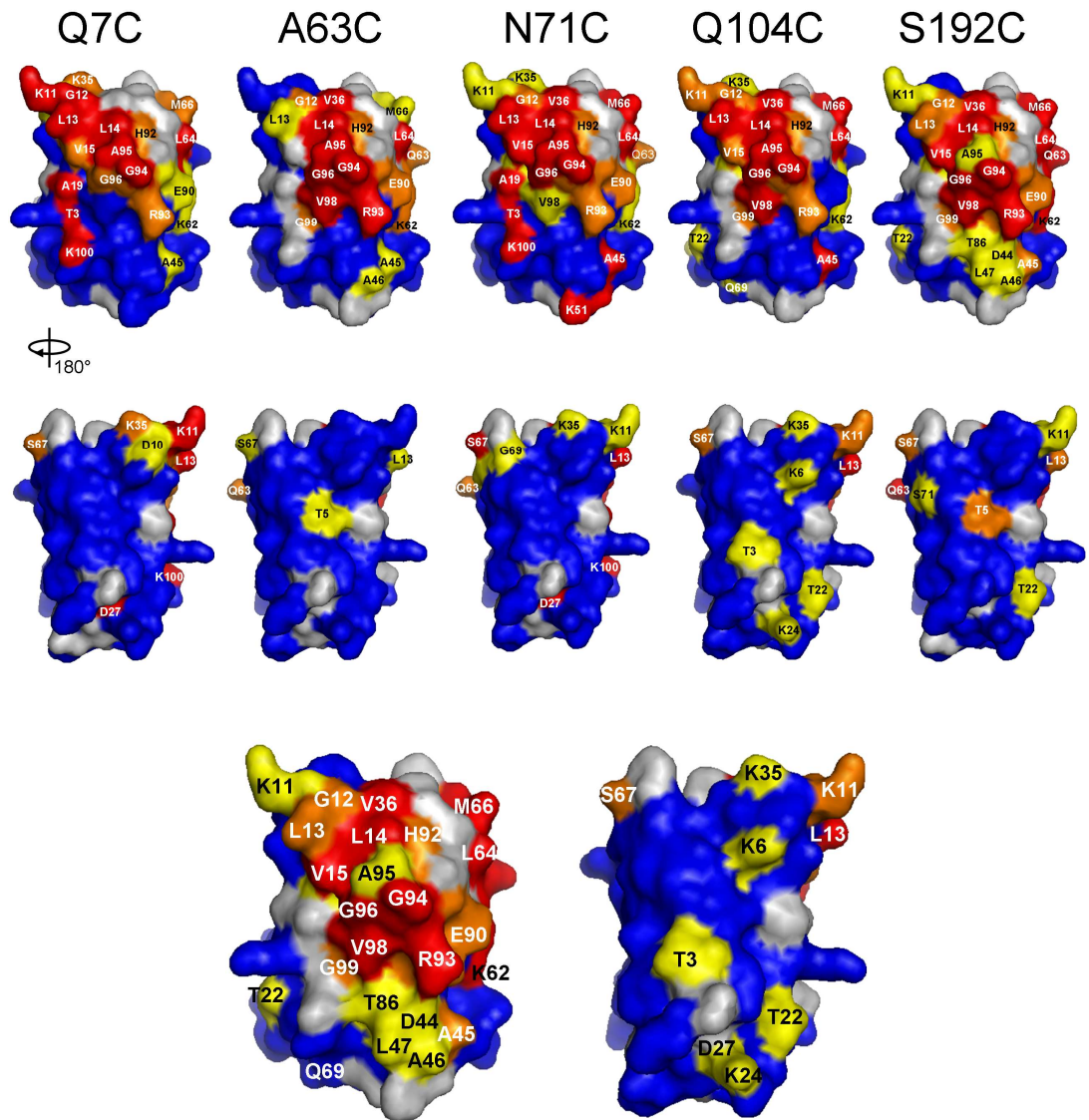
Figure 4.8 Surface representation of *Nostoc* Pc coloured according to $R_{2,para}$ observed in complex with the Cyt *f*-MTSL variant indicated at the top of the panel. The following classes have been used. Residues that disappear or experience a $R_{2,para} > 60/s^{-1}$ in red; $60\text{-}25/s^{-1}$ in orange; $25\text{-}15/s^{-1}$ in yellow; $<15/s^{-1}$ in blue. The residues for which no data are available are in grey. At the bottom, the S192C mutant (bottom left, front; bottom right, back) is shown enlarged for an easier reading of the name of the residues.

Comparing the PREs perturbation map of the Pc surface with the chemical shift perturbation map reported in the work of Diaz-Moreno and co-workers, a new region of the Pc appears to be affected

by the interaction with Cyt *f*. This is the lower region of Pc around residue A45 in A63C and especially in S192C (Figure 4.8, up). A similar perturbation is also detected for residue K24 in Q104C (Figure 4.8, bottom).

Structure calculation

Structure calculations were performed by Dr A. Volkov. The method used for the determination of the protein complex structure is based on the theory that the NMR resonance intensity of one of the proteins is influenced by a paramagnetic centre, for example a SL covalently attached to the partner protein. The unpaired electron on the SL produces an increase of the relaxation rate of nearby nuclei, because of the dipolar magnetic interactions induced between each nucleus and the SL. The influence of the paramagnetic centre depends on the inverse of the sixth power of the distance between the SL and the nucleus, averaged over all the positions adopted by the nuclei and the SL. The paramagnetic effects can then be converted into distance restraints[9,11] , which can be used to determine the relative orientation of the proteins[12]. Therefore, for every amide proton observed on Pc the PRE due to the MTSL has been determined, using the equation 4.1 [9,86]. From this equation R_2^{para} was obtained, so that the distance r could be obtained through the equation 4.2 [86]. This procedure has been applied to each of the five Cyt *f* mutants studied in this work in the complex with the Zn-Pc. The relaxation effect is very strong when the nuclei are in close proximity to the SL; under these conditions even lowly populated states, existing for only a small fraction of the lifetime of the complex, can be revealed. Still, it has to be considered that PRE data result from an average of the nuclear positions relative to the SL of both space and time. The structures that can be obtained, therefore, represent an average over all the adopted orientations[1].

In equation 4.2 τ_c is the rotational correlation time of the electron-nucleus vector. The total, effective rotational correlation time (τ_c) is determined by a contribution from the electron relaxation time τ_s and the rotational correlation time due to the tumbling of the molecule τ_r, according to $1/\tau_c = 1/\tau_s + 1/\tau_r$. In the case of proteins where the paramagnetic center is a stable radical $\tau_r < \tau_s$[75], therefore the value of τ_c is dominated by τ_r. The τ_c values used here were determined from the EPR spectra of each Cyt *f* mutant in the presence of Pc (Fig. 4.9) which were reported in the thesis of Dr. F. Scarpelli (Leiden University 2009). They are listed in Table 4.3[*].

---

[*] Subsequent studies have shown that it may be more appropriate to use τ_c for the entire complex[11]. However, the value of τ_c has been shown not to be critical[11]. For further details, see the concluding remarks of this chapter.
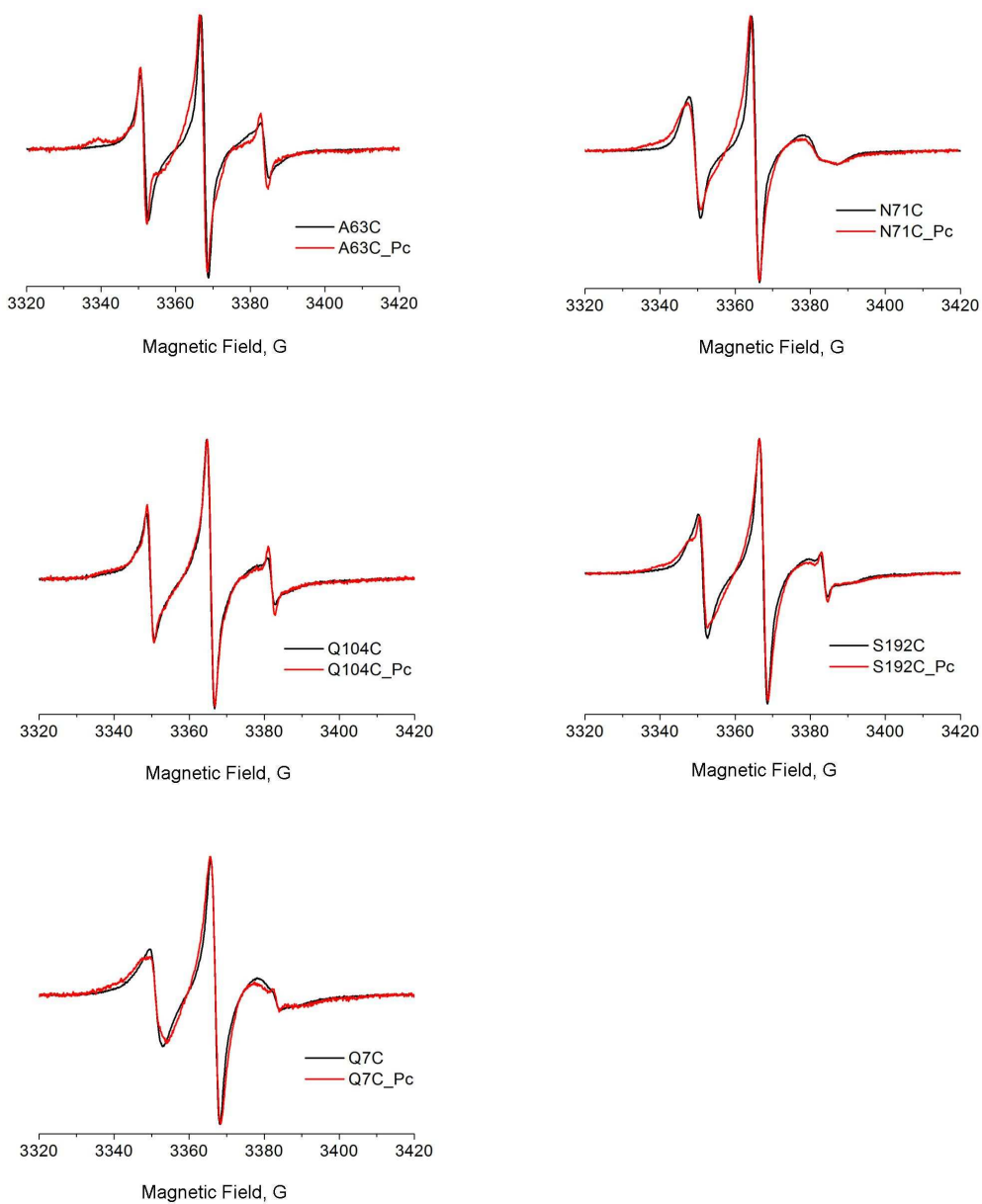
Figure 4.9 X band EPR at room temperature of the five mutated free Cyt *f* (black) and the corresponding Pc – Cyt *f* complexes (red).
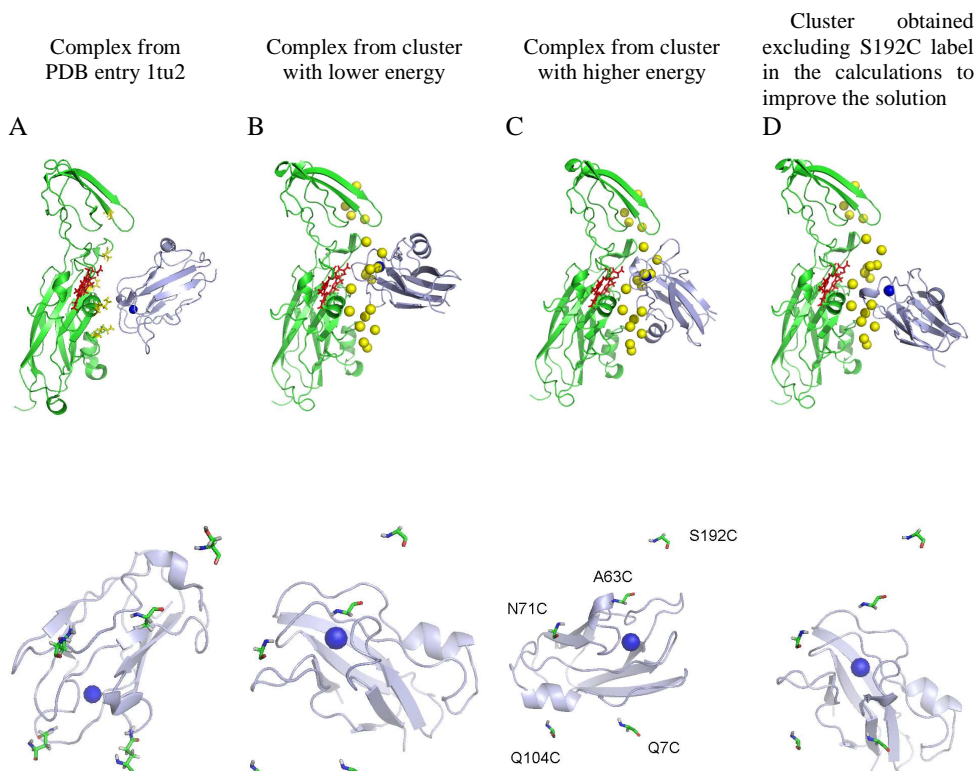
The intermolecular distance restraints obtained from the PRE between the measured position of the oxygen atom of MTSL and the backbone amide protons of Pc have been employed to determine the docking of Pc onto Cyt *f* and get independent information on the complex structure. A set of distance restraints for MTSL attached to five positions on Cyt *f* was used in a rigid-body docking protocol[11] with the aim to deduce the relative orientation of the two protein backbones in

the complex. Two low-energy clusters of Pc orientations separated by ca. 25 Å were found. Figure 4.10 B + C show the docking results for the case in which distance constraints from all 5 Cyt *f* variants are used. It is clear that both solutions differ significantly from the published orientation[56] (Figure 4.10, A). However, to value the relevance of the docking results, the agreement between the measurement and the back-predicted distances needs to be evaluated. The violation analysis of the solution structure (Figure 4.11) shows that many restraints are not satisfied.

***Table 4.3**. Rotational correlation time (τ_c, ns) for the spin label for each Cyt *f* mutant determined from EPR spectra

Cytochrome *f* mutant	Rotational correlation time (ns)
A63C	14
S192C	7
Q7C	6
Q104C	3
N71C	6

Complex from PDB entry 1tu2

Complex from cluster with lower energy

Complex from cluster with higher energy

Cluster obtained excluding S192C label in the calculations to improve the solution

A   B   C   D

Figure 4.10 Comparison of Cyt *f* – Pc relative orientations. Above: the whole complex. In A: the residues where the spin labels have been attached are indicated in yellow. In B, C and D: the yellow spheres represent the oxygen atom of the spin labels in the four chosen conformations. Below: detail of each complex obtained looking at the Pc from the Cyt *f* position.
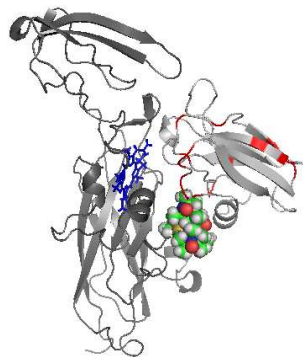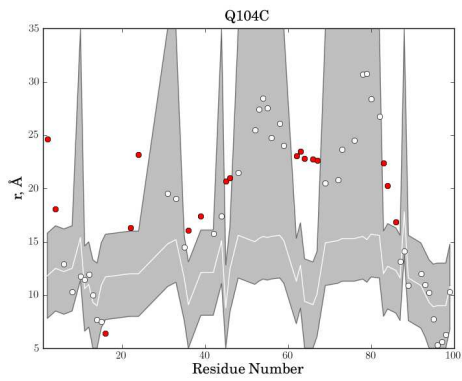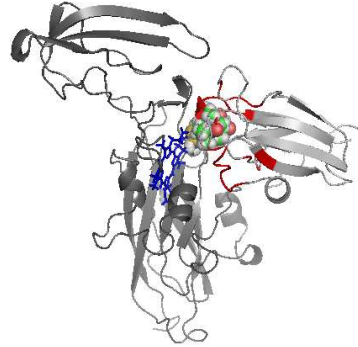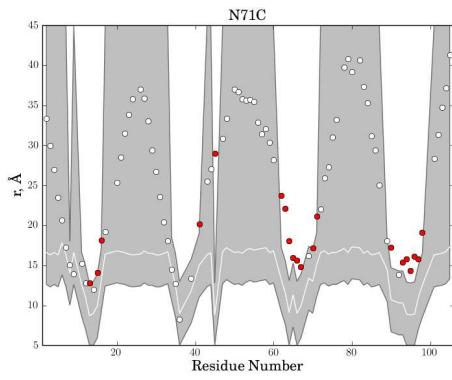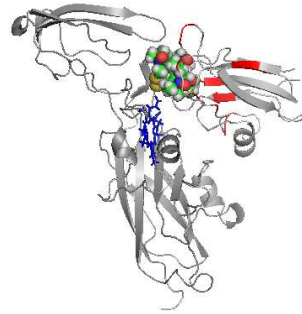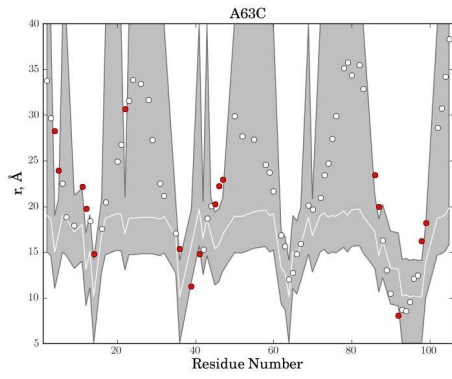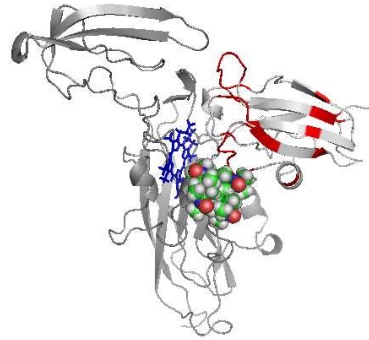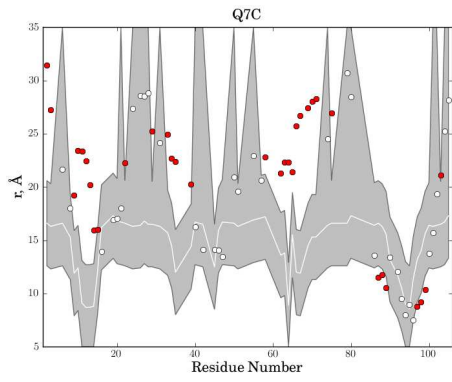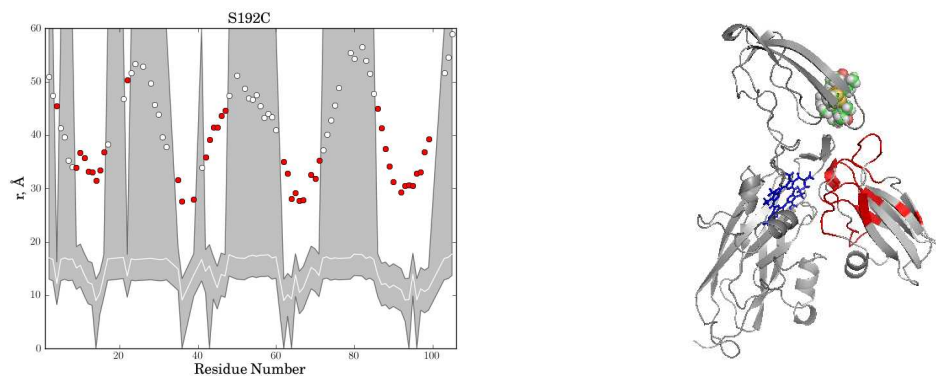
Figure 4.11 Violation analysis of the best structure solution for the Cyt *f* –Pc complex. The plots illustrate the distances from the Pc backbone amide protons in the best structure solution (circles) to the averaged position of the oxygen atom of MTSL attached to Cyt *f* at Q7C, A63C, N71C, Q104C and S192C positions. The white line and the shaded area indicate the PRE-derived distances and error margins, respectively, used in the structure calculations. Violations are represented as red circles. On the right cartoon representations of the best solution structure are shown, indicating the residues with satisfied (light gray) and violated (red) restraints. The haem group is in blue. For each of the MTSL positions, four conformations representing the freedom of the group are represented as spheres. These were used for ensemble averaging in the structure calculations.

The plots in Fig. 4.11 show the distances from the Pc backbone amide protons in the best solution structure (open circles) to the averaged position (calculated as explained in Materials and Methods) of the oxygen atom of MTSL attached to Cyt *f* for each of the Q7C, A63C, N71C, Q104C and S192C positions[11,88]. The white line and the shaded area indicate the PRE-derived distances and error margins, respectively, used in the structure calculations. For a given residue, the restraint is satisfied if the corresponding circle is inside the shaded area and violated if the circle is outside (red circles). The relative amount of violated restraints are similar for three mutants (16 % for A63C - Cyt *f* and Q104C - Cyt *f* ; 19 % for N71C). For the other two complexes, Q7C - Cyt *f* and S192C - Cyt *f*, the quantity of violated restraints is again similar (32 and 39 % respectively), and higher compared to the first group. For all variants, mainly positive violations are observed. Positive violations imply that the actual distances for residues in the single-orientation complex are larger than those determined experimentally.

The effects of leaving out the restraints of one spin label at a time during the docking calculations were studied. Only taking out the distant S192C label improved the quality of the fit, while for all other spin labels it did not make any difference, with many restraints yet to be satisfied. The orientation found (Fig. 4.10 D) is very similar to one of the solutions found with five SLs (Fig. 4.10 B). Then another spin label (in addition to S192C) was taken out. Runs with only 3 spin labels give solutions similar to the calculations excluding S192C only, irrespective of what spin labels were used. These observations suggest that it is not possible to meet all restraints in a single structure. Instead, the observed violations are evidence of additional protein-protein orientations sampled in the dynamic encounter state of the complex, in which the violated residues come close to the spin-

label. In that case, for each residue, the measured PRE (reflected in $R_{2,obs}^{para}$) is the sum of contributions from all protein-protein orientations (each contributing with R_2^{para}), weighted by the fraction of time (*f*) spent in each form, according to the equation 4.3[11], provided that all orientations are in fast exchange compared to the R_2^{para} values. Such an analysis was not performed in the present study.

$$R_{2,obs}^{para} = \sum_{i=1}^{n} f_i R_{2,i}^{para}$$ (Eq. 4.3)

In summary, the experimental results proved that the conformational search of Pc in the encounter complex extends further than just the region in the Cyt *f* nearby the interface of the well-defined complex found by Diaz-Moreno[56]. This is particularly evident looking at the perturbation map of the Pc bound to the S192C Cyt *f* mutant (see Figure 4.8). The sampled area resembles a valley in Cyt *f* situated between the small and big domains; this valley seems to be delineated by the five acidic residues (Asp-64, Glu-189, Asp-100, Glu-108 and Glu 165) that allow the electrostatic interactions with the positive groups of Pc. The hydrophobic patch of the Pc is oriented differently in cluster 1 and 2, but in both cases its edge is directed toward the Cyt *f* Tyr-1, like in the structure determined by Diaz-Moreno *et al*. Compared to this structure, in cluster 1 there is an additional positive electrostatic interaction between Lys-11 on Pc and Glu 189 in Cyt *f*, with the Cyt *f* Tyr-102 hydrophilic residue being very close to these two residues, while in the structure previously described it was found close to the hydrophobic patch. In cluster 2, the Pc K-51 and Cyt *f* D-100 residues are located in a way that makes it possible to form an additional electrostatic interaction between the two partner proteins, and also in this case Cyt *f* Tyr-102 is very close to these residues. In the Pc site 2 (indicated by light blue colour in Fig. 4.12), the Asp-54 and Lys-57 residues were found to be close to Cyt *f* E-189 by Diaz-Moreno. Here, they are more distant by it in cluster 1, but remain in the same region. In cluster 2, they are found between the E-108 and D-100 residues; in this latter case it seems that Pc is rotated by 180 degrees compared to the previous study, and that the hydrophobic patch is slid within the valley described above (Fig. 4.12, bottom), so that it is surrounded by the Cyt *f* E-189, K-35, E-165 acidic residues.

In order for the ET process to be fast enough (10^3-10^4 s^{-1}), the maximum distance between the redox centres should be in the order of 16 Å[91]. In the literature, in two plant complexes this distance was found to be 11.0 and 13.9 Å, while in the *Phormidium* complex it was 15.0 Å[56 and therein]. Our results show that the distance between Fe and Zn is 16.07 Å in cluster 1 (similar to the 16.1 Å previously found for *Nostoc* Cyt *f* – Cd Pc), and 14.1 Å in cluster 2. The structure described

here is therefore compatible with fast ET, although the distance in cluster 1 is close to the upper theoretical limit for efficient ET.
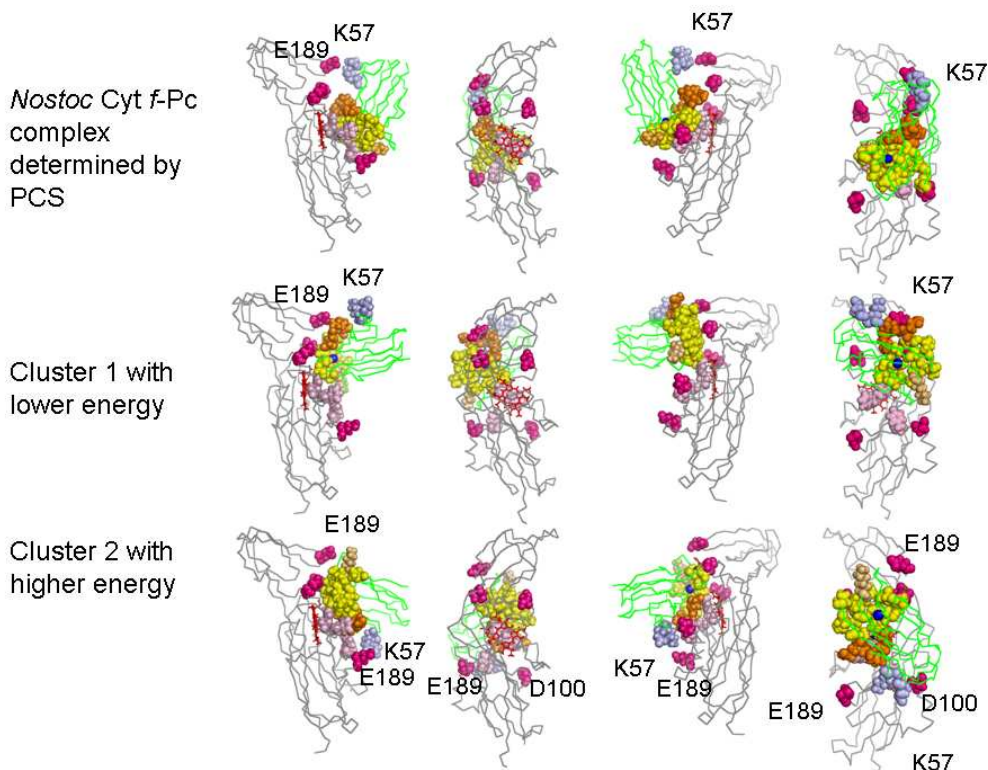
Figure 4.12 Comparison of Cyt *f* – Pc structures, obtained with PCS (top) and PRE NMR (middle and bottom). Pc and Cyt *f* are shown as green and grey ribbon, respectively; the five Cyt *f* acidic residues are in pink; the Pc hydrophobic patch is in yellow; the first electrostatic recognition site on Pc is in orange; the secondary recognition site on Pc is in light blue. On each row, the structure is observed through progressive 90 degrees rotations around the vertical axis.

Discussion

Previous studies to determine the orientation of Cd-plastocyanin (Pc-Cd) relative to Cyt *f* were performed[56] using chemical-shift perturbation data and intermolecular pseudo-contact shifts as experimental restraints, which were observed for the Pc amide nuclei and caused by the haem iron. The results showed that the hydrophobic patch, surrounding tyrosine 1 in Cyt *f*, docks the hydrophobic patch of Pc. The respective recognition sites of Cyt *f* and Pc give evidence for charge complementarities at the interface area. Further studies revealed that the binding affinity is independent of the oxidation state of Cyt *f*, but varies to some extent between Pc with a singly and doubly charged metal[56,65]. The interface map analysis showed a large perturbed area that, together with the localized nature of the binding map, indicates that the complex between Cyt *f* and Pc-Cd is well-defined, in agreement with the classification for "well defined" versus "dynamic" suggested by

Worrall *et al.*[8] and Prudencio and Ubbink[16]. Details about the conformation that the Pc assumes during most of the lifetime of the complex have been investigated; it was found that the orientation is the same as observed in plant complexes, rather than the one found for another cyanobacterial complex, that from *Phormidium*. The conclusion of that work, namely that in solution the proteins spend most of their time in a well-defined single-orientation complex, is in contrast with what was found in the present work. Here, the complex generated from the interaction of Cyt *f* and Pc in solution, investigated by the PRE NMR technique, cannot be explained by a single structure. In fact, all five Cyt *f* mutants prepared in the present study give similar results, which is unexpected for a complex with a single structure as proposed by Diaz-Moreno *et al.*[56].

This observation can be related to a particular step of the protein-protein interaction, the encounter complex. It should be underlined that kinetic studies of the *Nostoc* Cyt *f*-Pc complex by Albarran *et al.*, in which the effects of mutations on the kinetics of electron transfer to wild-type and mutant forms of Pc were measured by laser flash absorption spectroscopy, showed that a wide area is involved in the electrostatic interaction with Pc in the complex; this was explained to be the result of an additive effect of multiple specific interactions[71]. This observation is in agreement with our hypothesis. In fact, the results of the present work also suggest that the orientation of the two proteins in the complex is such that Pc searches the negatively charged, long face of Cyt *f,* while being aligned along its long axis, exploring a large Cyt *f* surface always with the same area. Proteins, and macromolecules in general, recognize partners through short-range biophysical interactions, like hydrogen bonding, hydrophobic and van der Waals forces at the binding interface, usually representing only a small fraction of the total surface of the protein[1]. The process of complex formation involves two phases. In the first, the protein meets its partner and forms a transient intermediate involving non-specific binding modes, which is a dynamic encounter state that produces the encounter complex. The latter may then follow two paths, forming the final complex or dissociating again[1]. Suh *et al.* stressed the importance of electrostatic interactions in the initial phase of the protein formation[19]; in the same work it was shown that distinguishing between specific and non-specific conformations may be difficult, due to the small energy difference between the two.

The results of the present work, although different from what was published by Diaz-Moreno, are not incompatible with it: due to the PRE technique used in this work, we were able to detect ensembles of sparsely populated conformations that contribute to the encounter complex of the two proteins. This conclusion is in line with recent studies performed on protein dynamics[1]. In particular, it was found that proteins may form an entirely dynamic complex, like that between adrenoxin and cytochrome *c*[15]. Although it is generally difficult to crystallize ET complexes, this

has been possible for cytochrome *c* and cytochrome *c* peroxidase from yeast. Since the crystallized complex was ET active, this suggested that the complex was fully specific. In contrast, it was recently found that only 70% of the complex is well-defined, with 30% representing the encounter complex[11,23]. Similar results have been reported by Tang *et al.* on other protein complexes[12].

Concluding remarks

The experimental data are best interpreted by the presence of a dynamic ensemble of protein-proteins orientations within the complex rather than a single, well-defined structure. Perhaps the most important result of the present work is that the effects observed with the PRE technique cannot be modelled by a single structure. This conclusion will not be affected by the choice of different τ_c values for the different mutants as discussed in detail by Volkov *et al.*[11]. In fact, the comparison made by these authors shows that the exact correlation time used is not critical. However, structure calculations should be performed with the τ_c of the complex.

Visualizing an encounter complex is a complex task, since this involves taking into account non-specific interactions and dynamics, leading to many orientations. Future work is needed, and a promising possibility is to associate experimental data with computational dynamics to provide more detailed insights into the nature of protein complex formation, of which the encounter complex is an important part.

Reference List

1. Ubbink,M. The courtship of proteins: Understanding the encounter complex. *Febs Letters* **583**, 1060-1066 (2009).

2. Ubbink,M., Ejdeback,M. & Karlsson,B.G. The structure of the complex of plastocyanin and cytochrome *f*, determined by paramagnetic NMR and restrained rigid-body molecular dynamics. *Structure* **6**, 323-335 (1998).

3. Hoffman,B.M., Celis,L.M., Cull,D.A., Patel,A.D., Seifert,J.L., Wheeler,K.E., Wang,J.Y., Yao,J., Kurnikov,I.V. & Nocek,J.M. Differential influence of dynamic processes on forward and reverse electron transfer across a protein-protein interface. *Proceedings of the National Academy of Sciences of the United States of America* **102**, 3564-3569 (2005).

4. Crowley,P.B., Otting,G., Schlarb-Ridley,B.G., Canters,G.W. & Ubbink,M. Hydrophobic interactions in a cyanobacterial plastocyanin-cytochrome *f* complex. *Journal of the American Chemical Society* **123**, 10444-10453 (2001).

5. Garrett,D.S., Seok,Y.J., Peterkofsky,A., Gronenborn,A.M. & Clore,G.M. Solution structure of the 40,000 M-r phosphoryl transfer complex between the N-terminal domain of enzyme I and HPr. *Nature Structural Biology* **6**, 166-173 (1999).

6. Worrall,J.A.R., Reinle,W., Bernhardt,R. & Ubbink,M. Transient protein interactions studied by NMR spectroscopy: The case of cytochrome *c* and adrenodoxin. *Biochemistry* **42**, 7068-7076 (2003).

7. Liang,Z.X., Jiang,M., Ning,Q. & Hoffman,B.M. Dynamic docking and electron transfer between myoglobin and cytochrome b_5. *Journal of Biological Inorganic Chemistry* **7**, 580-588 (2002).

8. Worrall,J.A.R., Liu,Y.J., Crowley,P.B., Nocek,J.M., Hoffman,B.M. & Ubbink,M. Myoglobin and cytochrome b_5: A nuclear magnetic resonance study of a highly dynamic protein complex. *Biochemistry* **41**, 11721-11730 (2002).

9. Liang,Z.X., Nocek,J.M., Huang,K., Hayes,R.T., Kurnikov,I.V., Beratan,D.N. & Hoffman,B.M. Dynamic docking and electron transfer between Zn-myoglobin and cytochrome b_5. *Journal of the American Chemical Society* **124**, 6849-6859 (2002).

10. Volkov,A.N., Ferrari,D., Worrall,J.A.R., Bonvin,A.M.J.J. & Ubbink,M. The orientations of cytochrome *c* in the highly dynamic complex with cytochrome b_5 visualized by NMR and docking using HADDOCK. *Protein Science* **14**, 799-811 (2005).

11. Volkov,A.N., Worrall,J.A.R., Holtzmann,E. & Ubbink,M. Solution structure and dynamics of the complex between cytochrome *c* and cytochrome *c* peroxidase determined by paramagnetic NMR. *Proceedings of the National Academy of Sciences of the United States of America* **103**, 18945-18950 (2006).

12. Tang,C., Iwahara,J. & Clore,G.M. Visualization of transient encounter complexes in protein-protein association. *Nature* **444**, 383-386 (2006).

13. Iwahara,J. & Clore,G.M. Detecting transient intermediates in macromolecular binding by paramagnetic NMR. *Nature* **440**, 1227-1230 (2006).

14. Xu,X.F., Keizers,P.H.J., Reinle,W., Hannemann,F., Bernhardt,R. & Ubbink,M. Intermolecular dynamics studied by paramagnetic tagging. *Journal of Biomolecular NMR* **43**, 247-254 (2009).

15. Xu,X.F., Reinle,W.G., Hannemann,F., Konarev,P.V., Svergun,D.I., Bernhardt,R. & Ubbink,M. Dynamics in a pure encounter complex of two proteins studied by solution scattering and paramagnetic NMR spectroscopy. *Journal of the American Chemical Society* **130**, 6395-6403 (2008).

16. Prudencio,M. Transient complexes of redox proteins: structural and dynamic details from NMR studies. *Journal of Molecular Recognition* **17**, 524-539 (2004).

17. Fawzi,N.L., Doucleff,M., Suh,J.Y. & Clore,G.M. Mechanistic details of a protein-protein association pathway revealed by paramagnetic relaxation enhancement titration measurements. *Proceedings of the National Academy of Sciences of the United States of America* **107**, 1379-1384 (2010).

18. Harel,M., Spaar,A. & Schreiber,G. Fruitful and futile encounters along the association reaction between proteins. *Biophysical Journal* **96**, 4237-4248 (2009).

19. Suh,J.Y., Tang,C. & Clore,G.M. Role of electrostatic interactions in transient encounter complexes in protein-protein association investigated by paramagnetic relaxation enhancement. *Journal of the American Chemical Society* **129**, 12954-12955 (2007).

20. Kim,Y.C., Tang,C., Clore,G.M. & Hummer,G. Replica exchange simulations of transient encounter complexes in protein-protein association. *Proceedings of the National Academy of Sciences of the United States of America* **105**, 12855-12860 (2008).

21. Northrup,S.H., Boles,J.O. & Reynolds,J.C.L. Brownian dynamics of cytochrome *c* and cytochrome *c* peroxidase association. *Science* **241**, 67-70 (1988).

22. Volkov,A.N., Bashir,O., Worrall,J.A.R. & Ubbink,M. Binding hot spot in the weak protein complex of physiological redox partners yeast cytochrome *c* and cytochrome *c* peroxidase. *Journal of Molecular Biology* **385**, 1003-1013 (2009).

23. Bashir,Q., Volkov,A.N., Ullmann,G.M. & Ubbink,M. Visualization of the encounter ensemble of the transient electron transfer complex of cytochrome *c* and cytochrome *c* peroxidase. *Journal of the American Chemical Society* **132**, 241-247 (2010).

24. Adam,G. & Delbruck,M. Structural Chemistry and Molecular Biology. Freeman, San Francisco, (1968).

25. Volkov, A. Transient Complexes of Haem Proteins. Ph.D. thesis. Leiden University, Leiden, The Netherlands, 2007

26. Northrup,S.H. & Erickson,H.P. Kinetics of protein protein association explained by Brownian dynamics computer simulation. *Proceedings of the National Academy of Sciences of the United States of America* **89**, 3338-3342 (1992).

27. Radic,Z., Kirchhoff,P.D., Quinn,D.M., McCammon,J.A. & Taylor,P. Electrostatic influence on the kinetics of ligand binding to acetylcholinesterase - Distinctions between active center ligands and fasciculin. *Journal of Biological Chemistry* **272**, 23265-23277 (1997).

28. Schreiber,G. & Fersht,A.R. Rapid, electrostatically assisted association of proteins. *Nature Structural Biology* **3**, 427-431 (1996).

29. Smoluchowski,M.V. Veruch einer mathematischen theorie der koagulationkinetik kolloider losungen. *Z. Phys. Chem* 129-168 (1917).

30. Crowley, P. B. Transient Protein Interactions of Photosynthetic Redox Partners. Ph.D. thesis. Leiden University, Leiden, The Netherlands, 2002

31. Crowley,P.B. & Ubbink,M. Close encounters of the transient kind: Protein interactions in the photosynthetic redox chain investigated by NMR spectroscopy. *Accounts of Chemical Research* **36**, 723-730 (2003).

32. Crowley,P.B. & Carrondo,M.A. The architecture of the binding site in redox protein complexes: Implications for fast dissociation. *Proteins-Structure Function And Bioinformatics* **55**, 603-612 (2004).

33. Kurisu,G., Zhang,H.M., Smith,J.L. & Cramer,W.A. Structure of the cytochrome b_6f complex of oxygenic photosynthesis: Tuning the cavity. *Science* **302**, 1009-1014 (2003).

34. Nelson,N. & Ben Shem,A. The complex architecture of oxygenic photosynthesis. *Nature Reviews Molecular Cell Biology* **5**, 971-982 (2004).

35. Kruse,O., Rupprecht,J., Mussgnug,J.R., Dismukes,G.C. & Hankamer,B. Photosynthesis: a blueprint for solar energy capture and biohydrogen production technologies. *Photochemical & Photobiological Sciences* **4**, 957-970 (2005).

36. Noy,D., Moser,C.C. & Dutton,P.L. Design and engineering of photosynthetic light-harvesting and electron transfer using length, time, and energy scales. *Biochimica Et Biophysica Acta-Bioenergetics* **1757**, 90-105 (2006).

37. Iverson,T.M. Evolution and unique bioenergetic mechanisms in oxygenic photosynthesis. *Current Opinion in Chemical Biology* **10**, 91-100 (2006).

38. Martinez,S.E., Huang,D., Szczepanink,A. & Cramer,W.A. Crystal-structure of chloroplast cytochrome *f* reveals a novel cytochrome fold and unexpected heme ligation. *Structure* **2**, 95-105 (1994).

39. Sandmann,G. Formation of plastocyanin and cytochrome c_{553} in different species of blue-green algae. *Archives of Microbiology* **145**, 76-79 (1986).

40. Merchant,S., Hill,K. & Howe,G. Dynamic interplay between 2 copper-titrating components in the transcriptional regulation of cyt c_6. *Embo Journal* **10**, 1383-1389 (1991).

41. Bovy,A., Devrieze,G., Borrias,M. & Weisbeek,P. Transcriptional regulation of the plastocyanin and cytochrome c_{553} genes from the cyanobacterium *Anabaena* species PCC 7937. *Molecular Microbiology* **6**, 1507-1513 (1992).

42. Zhang,L., Mcspadden,B., Pakrasi,H.B. & Whitmarsh,J. Copper-mediated regulation of cytochrome c_{553} and plastocyanin in the cyanobacterium *Synechocystis* 6803. *Journal of Biological Chemistry* **267**, 19054-19059 (1992).

43. Navarro,J.A., Hervas,M. & DelaRosa,M.A. Co-evolution of cytochrome c_6 and plastocyanin, mobile proteins transferring electrons from cytochrome b_6f to photosystem I. *Journal of Biological Inorganic Chemistry* **2**, 11-22 (1997).

44. Gross,E.L. & Pearson,D.C. Brownian dynamics simulations of the interaction of *Chlamydomonas* cytochrome *f* with plastocyanin and cytochrome c_6. *Biophysical Journal* **85**, 2055-2068 (2003).

45. Bendall,D.S. Interprotein electron transfer in Protein Electron Transfer , Bendall,D.S. (ed.) pp. 43-64 (BIOS Scientific Publishers Ltd.,Oxford,1996).

46. Kannt,A., Young,S. & Bendall,D.S. The role of acidic residues of plastocyanin in its interaction with cytochrome *f*. *Biochimica Et Biophysica Acta-Bioenergetics* **1277**, 115-126 (1996).

47. Soriano,G.M., Ponamarev,M.V., Tae,G.S. & Cramer,W.A. Effect of the interdomain basic region of cytochrome *f* on its redox reactions in vivo. *Biochemistry* **35**, 14590-14598 (1996).

48. Hope,A.B. Electron transfers amongst cytochrome *f*, plastocyanin and photosystem I: kinetics and mechanisms. *Biochimica Et Biophysica Acta-Bioenergetics* **1456**, 5-26 (2000).

49. Lange,C., Cornvik,T., Diaz-Moreno,I. & Ubbink,M. The transient complex of poplar plastocyanin with cytochrome *f*: effects of ionic strength and pH. *Biochimica Et Biophysica Acta-Bioenergetics* **1707**, 179-188 (2005).

50. Niwa,S., Ishikawa,H., Nikai,S. & Takabe,T. Electron-transfer reactions between cytochrome *f* and plastocyanin from *Brassica komatsuna*. *Journal of Biochemistry* **88**, 1177-1183 (1980).

51. Takenaka,K. & Takabe,T. Importance of local positive charges on cytochrome *f* for electron transfer to plastocyanin and potassium ferricyanide. *Journal of Biochemistry* **96**, 1813-1821 (1984).

52. Beokubetts,D., Chapman,S.K., Knox,C.V. & Sykes,A.G. Kinetic studies on 1:1 electron-transfer reactions involving blue copper proteins. 11. Effects of pH, competitive inhibition, and Chromium(III) modification on the reaction of plastocyanin with cytochrome *f*. *Inorganic Chemistry* **24**, 1677-1681 (1985).

53. Takabe,T. & Ishikawa,H. Kinetic studies on a cross-linked complex between plastocyanin and cytochrome *f*. *Journal of Biochemistry* **105**, 98-102 (1989).

54. Zhou,J.H., FernandezVelasco,J.G. & Malkin,R. N-terminal mutants of chloroplast cytochrome *f* - Effect on redox reactions and growth in *Chlamydomonas reinhardtii*. *Journal of Biological Chemistry* **271**, 6225-6232 (1996).

55. Hart,S.E., Schlarb-Ridley,B.G., Delon,C., Bendall,D.S. & Howe,C.J. Role of charges on cytochrome *f* from the cyanobacterium *Phormidium laminosum* in its interaction with plastocyanin. *Biochemistry* **42**, 4829-4836 (2003).

56. Diaz-Moreno,I., Diaz-Quintana,A. & De la Rosa,M.A. Structure of the complex between plastocyanin and cytochrome *f* from the cyanobacterium *Nostoc* sp PCC 7119 as determined by paramagnetic NMR - The balance between electrostatic and hydrophobic interactions within the transient complex determines the relative orientation of the two proteins. *Journal of Biological Chemistry* **280**, 18908-18915 (2005).

57. Gross,E.L. & Rosenberg,I. A brownian dynamics study of the interaction of *Phormidium* cytochrome *f* with various cyanobacterial plastocyanins. *Biophysical Journal* **90**, 366-380 (2006).

58. Hulsker,R., Baranova,M.V., Bullerjahn,G.S. & Ubbink,M. Dynamics in the transient complex of plastocyanin-cytochrome *f* from *Prochlorothrix hollandica*. *Journal of the American Chemical Society* **130**, 1985-1991 (2008).

59. Qin,L. & Kostic,N.M. Electron-transfer reactions of cytochrome *f* with flavin semiquinones and with plastocyanin - Importance of protein-protein electrostatic interactions and of donor-acceptor coupling. *Biochemistry* **31**, 5145-5150 (1992).

60. DeLano, W. L. The PyMOL Molecular Graphics System, http://www.pymol.org (2002)

61. O'Connell,M.R., Gamsjaeger,R. & Mackay,J.P. The structural analysis of protein-protein interactions by NMR spectroscopy. *Proteomics* **9**, 5224-5232 (2009).

62. Gray,J.C. Cytochrome *f* - Structure, function and biosynthesis. *Photosynthesis Research* **34**, 359-374 (1992).

63. Hervas,M., Navarro,J.A. & De la Rosa,M.A. Electron transfer between membrane complexes and soluble proteins in photosynthesis. *Accounts of Chemical Research* **36**, 798-805 (2003).

64. De la Rosa,M.A., Molina-Heredia,F.P., Hervas,M. & Navarro,J.A. Convergent evolution of plastocyanin and cytochrome c_6 in Photosystem I: The light-driven, plastocyanin: ferredoxin oxidoreductase, Golbeck,J.H. (ed.) pp. 683-696 (Springer, New York,2006).

65. Diaz-Moreno,I., Diaz-Quintana,A., De la Rosa,M.A., Crowley,P.B. & Ubbink,M. Different modes of interaction in cyanobacterial complexes of plastocyanin and cytochrome *f*. *Biochemistry* **44**, 3176-3183 (2005).

66. Schmidt,L., Christensen,H.E.M. & Harris,P. Structure of plastocyanin from the cyanobacterium *Anabaena variabilis*. *Acta Crystallographica Section D-Biological Crystallography* **62**, 1022-1029 (2006).

67. Albarran,C., Navarro,J.A. & De la Rosa,M.A. The specificity in the interaction between cytochrome *f* and plastocyanin from the cyanobacterium *Nostoc* sp. PCC 7119 is mainly determined by the copper protein. *Biochemistry* **46**, 997-1003 (2007).

68. Jones,S. & Thornton,J.M. Analysis of protein-protein interaction sites using surface patches. *Journal of Molecular Biology* **272**, 121-132 (1997).

69. Chakrabarti,P. & Janin,J. Dissecting protein-protein recognition sites. *Proteins-Structure Function and Genetics* **47**, 334-343 (2002).

70. Janin,J. & Wodak,S.J. Protein modules and protein-protein interaction - Introduction. *Advances in Protein Chemistry* **61**, 1-8 (2003).

71. Albarran,C., Navarro,J.A., Molina-Heredia,F.P., Murdoch,P.S., De la Rosa,M.A. & Hervas,M. Laser flash-induced kinetic analysis of cytochrome *f* oxidation by wild-type and mutant plastocyanin from the cyanobacterium *Nostoc* sp. PCC 7119. *Biochemistry* **44**, 11601-11607 (2005).

72. Molina-Heredia,F.P., Hervas,M., Navarro,J.A. & De la Rosa,M.A. A single arginyl residue in plastocyanin and in cytochrome c_6 from the cyanobacterium *Anabaena* sp. PCC 7119 is required for efficient reduction of photosystem I. *Journal of Biological Chemistry* **276**, 601-605 (2001).

73. Vlasie,M.D., Fernandez-Busnadiego,R., Prudencio,M. & Ubbink,M. Conformation of pseudoazurin in the 152 kDa electron transfer complex with nitrite reductase determined by paramagnetic NMR. *Journal of Molecular Biology* **375**, 1405-1415 (2008).

74. Ubbink,M. & Bendall,D.S. Complex of plastocyanin and cytochrome *c* characterized by NMR chemical shift analysis. *Biochemistry* **36**, 6326-6335 (1997).

75. Keizers,P.H.J. & Ubbink,M. Paramagnetic tagging for protein structure and dynamics analysis. *Progress in Nuclear Magnetic Resonance Spectroscopy* **58**, 88-96 (2011).

76. Iwahara,J., Zweckstetter,M. & Clore,G.M. NMR structural and kinetic characterization of a homeodomain diffusing and hopping on nonspecific DNA. *Proceedings of the National Academy of Sciences of the United States of America* **103**, 15062-15067 (2006).

77. Hulsker, R. Transient interactions between photosynthetic proteins. Ph.D. thesis. Leiden University, Leiden, The Netherlands, 2008

78. Milikisyants,S., Scarpelli,F., Finiguerra,M.G., Ubbink,M. & Huber,M. A pulsed EPR method to determine distances between paramagnetic centers with strong spectral anisotropy and radicals: The dead-time free RIDME sequence. *Journal of Magnetic Resonance* **201**, 48-56 (2009).

79. Thony-Meyer,L. Haem-polypeptide interactions during cytochrome *c* maturation. *Biochimica Et Biophysica Acta-Bioenergetics* **1459**, 316-324 (2000).

80. Neu,H.C. & Heppel,L.A. The release of enzymes from *Escherichia Coli* by osmotic shock and during formation of spheroplasts. *Journal of Biological Chemistry* **240**, 3685-3692 (1965).

81. Molina-Heredia,F.P., Hervas,M., Navarro,J.A. & De la Rosa,M.A. Cloning and correct expression in *Escherichia coli* of the petE and petJ genes respectively encoding plastocyanin and cytochrome c_6 from the cyanobacterium *Anabaena* sp. PCC 7119. *Biochemical and Biophysical Research Communications* **243**, 302-306 (1998).

82. Ubbink,M., Lian,L.Y., Modi,S., Evans,P.A. & Bendall,D.S. Analysis of the H-1-NMR chemical shifts of Cu(I)-, Cu(II)- and Cd-substituted pea plastocyanin - Metal-dependent differences in the hydrogen-bond network around the copper site. *European Journal of Biochemistry* **242**, 132-147 (1996).

83. Boucher, W. AZARA 2.7, www.bio.cam.ac.uk/pub/azara (2002)

84. Helgstrand,M., Kraulis,P., Allard,P. & Hard,T. Ansig for Windows: An interactive computer program for semiautomatic assignment of protein NMR spectra. *Journal of Biomolecular NMR* **18**, 329-336 (2000).

85. Kraulis,P.J. Ansig - A program for the assignment of protein H-1 2D-NMR spectra by interactive computer-graphics. *Journal of Magnetic Resonance* **84**, 627-633 (1989).

86. Battiste,J.L. Utilization of site-directed spin labeling and high-resolution heteronuclear nuclear magnetic resonance for global fold determination of large proteins with limited nuclear overhauser effect data. *Biochemistry* **39**, 5355-5365 (2000).

87. Schwieters,C.D., Kuszewski,J.J., Tjandra,N. & Clore,G.M. The Xplor-NIH NMR molecular structure determination package. *Journal of Magnetic Resonance* **160**, 65-73 (2003).

88. Iwahara,J., Schwieters,C.D. & Clore,G.M. Ensemble approach for NMR structure refinement against H-1 paramagnetic relaxation enhancement data arising from a flexible paramagnetic group attached to a macromolecule. *Journal of the American Chemical Society* **126**, 5879-5896 (2004).

89. Hubbell,W.L., Mchaourab,H.S., Altenbach,C. & Lietzow,M.A. Watching proteins move using site-directed spin labeling. *Structure* **4**, 779-783 (1996).

90. Liang,B.Y., Bushweller,J.H. & Tamm,L.K. Site-directed parallel spin-labeling and paramagnetic relaxation enhancement in structure determination of membrane proteins by solution NMR spectroscopy. *Journal of the American Chemical Society* **128**, 4389-4397 (2006).

91. Moser,C.C., Keske,J.M., Warncke,K., Farid,R.S. & Dutton,P.L. Nature of biological electron-transfer. *Nature* **355**, 796-802 (1992).